Ph 21.2 - Introduction to Fourier Transforms

Yovan Badal

04/14/2018

1 Properties and Consistency of the Fourier Series

1. We prove the consistency of eqns (2) and (3) as respective definitions of the inverse Fourier series and Fourier series.

$$\sum_{k=-\infty}^{\infty} \tilde{h}_k e^{-2\pi i f_k x} = \sum_{k=-\infty}^{\infty} e^{-2\pi i f_k x} \frac{1}{L} \int_0^L h(x') e^{2\pi i f_k x'} \, \mathrm{d}x' \tag{1}$$

$$= \int_0^L \sum_{k=-\infty}^{\infty} \frac{1}{L} h(x') e^{-2\pi i \frac{k}{L}(x'-x)} \, \mathrm{d}x' \tag{2}$$

$$= \int_{-\infty}^{-\infty} \int_{-\infty}^{\infty} \frac{1}{L} h(x') e^{-2\pi i \frac{k}{L}(x'-x)} \, \mathrm{d}k \, \mathrm{d}x' \tag{3}$$

$$= \int_{-\infty}^{-\infty} h(x') \int_{-\infty}^{\infty} e^{-2\pi i k'(x'-x)} \, \mathrm{d}k' \, \mathrm{d}x' \tag{4}$$

$$= \int_{-\infty}^{-\infty} h(x') \delta(x'-x) \, \mathrm{d}x' \tag{5}$$

$$= h(x) \tag{6}$$

where in line (3) we change the bounds of our x-integral by setting for convenience our function $h(x)$ to be 0 outside of $x \in [0, L)$ and we use the fact that the signal we are concerned with is periodic to replace the infinite sum over k with an indefinite k-integral. This is because the Fourier *transform*, given by $H(k) = \int_{-\infty}^{\infty} h(x) e^{2\pi i k x} \, \mathrm{d}x$ (an extension of sorts of the Fourier series used to analyze aperiodic signals) of a periodic signal $h(x)$ consists of a sum of delta-distributions, which reduces the integral $H(k)$ to an infinte sum of complex exponetials over integer k. In line (4), we use a simple change of variables, in line (5) we use the Fourier transform of the dirac-delta distribution, and in line (6) we use the fundamental property of the dirac-delta distribution.

2. We work out a special case of the completeness of complex exponentials.

$$A\sin(2\pi x/L+\varphi) = \frac{iA}{2}(e^{-i(2\pi x/L+\varphi)} - e^{i(2\pi x/L+\varphi)}) \tag{7}$$
$$= \frac{iA}{2}\big(e^{-i\varphi}e^{-2\pi ix/L} - e^{i\varphi}e^{2\pi ix/L}\big) \tag{8}$$
$$= \left(\frac{iA}{2}e^{-i\varphi}\right)e^{-2\pi ix/L} - \left(\frac{iA}{2}e^{i\varphi}\right)e^{2\pi ix/L} \tag{9}$$

where in line (7) we have used DeMoivre's theorem. This proves the claim.

3. We demonstrate a property of the Fourier coefficients for real $h(x)$.

$$\tilde{h}_{-k} = \frac{1}{L}\int_0^L h(x)e^{2\pi i f_{-k}x}\,\mathrm{d}x \tag{10}$$
$$=\frac{1}{L}\int_0^L h(x)e^{-2\pi i f_k x}\,\mathrm{d}x \tag{11}$$
$$=\frac{1}{L}\int_0^L h(x)\big[e^{2\pi i f_k x}\big]^*\,\mathrm{d}x \tag{12}$$
$$=\left[\frac{1}{L}\int_0^L h(x)e^{2\pi i f_k x}\,\mathrm{d}x\right]^* \tag{13}$$
$$=\tilde{h}_k^* \tag{14}$$

where in line (11) we have used the definition $f_k = \frac{k}{L}$, in line (12) we have used an obvious property of the complex exponential (which can easily be seen using DeMoivre's theorem) and in line (13) we have used the fact that $h(x)$ and our integration variable x are real.

4. We prove a version of the convolution theorem for Fourier series. Let $H(x) = h^{(1)}(x)h^{(2)}(x)$. Then we can write the Fourier series for $h^{(1)}(x)$ and $h^{(2)}(x)$:

$$h^{(1)}(x) = \sum_{k=-\infty}^{\infty}\tilde{h}_k^{(1)}e^{-2\pi i f_k x} \tag{15}$$
$$h^{(2)}(x) = \sum_{k=-\infty}^{\infty}\tilde{h}_k^{(2)}e^{-2\pi i f_k x} \tag{16}$$

such that we can write $H(x)$ as:

$$H(x) =h^{(1)}(x)h^{(2)}(x) \tag{17}$$
$$=\left(\sum_{k=-\infty}^{\infty}\tilde{h}_k^{(1)}e^{-2\pi i f_k x}\right)\left(\sum_{k=-\infty}^{\infty}\tilde{h}_k^{(2)}e^{-2\pi i f_k x}\right) \tag{18}$$
$$= \sum_{k=-\infty}^{-\infty}\left(\sum_{k'=-\infty}^{\infty}\tilde{h}_{k-k'}^{(1)}\tilde{h}_{k'}^{(2)}\right)e^{-2\pi i f_k x} \tag{19}$$

and we can then find the Fourier coefficents H_k of $H(x)$ as follows:

$$H_k = \frac{1}{L}\int_0^L H(x)e^{2\pi i f_k x}\,\mathrm{d}x \tag{20}$$

$$= \frac{1}{L}\int_0^L \sum_{l=-\infty}^{\infty}\left(\sum_{k'=-\infty}^{\infty}\tilde{h}^{(1)}_{l-k'}\tilde{h}^{(2)}_{k'}\right)e^{-2\pi i f_l x}e^{2\pi i f_k x}\,\mathrm{d}x \tag{21}$$

$$= \frac{1}{L}\int_0^L \sum_{l=-\infty}^{\infty}\left(\sum_{k'=-\infty}^{\infty}\tilde{h}^{(1)}_{l-k'}\tilde{h}^{(2)}_{k'}\right)e^{2\pi i (f_k - f_l) x}\,\mathrm{d}x \tag{22}$$

$$= \frac{1}{L}\sum_{l=-\infty}^{\infty}\left(\sum_{k'=-\infty}^{\infty}\tilde{h}^{(1)}_{l-k'}\tilde{h}^{(2)}_{k'}\right)\int_0^L e^{2\pi i (f_k - f_l) x}\,\mathrm{d}x \tag{23}$$

$$\tag{24}$$

Now, observe that $\int_0^L e^{2\pi i(f_k - f_l)x}\,\mathrm{d}x = \begin{cases} L & k=l \\ 0 & \text{else} \end{cases}$ since we are integrating over an integer number of periods of the complex exponential. Therefore:

$$H_k = \sum_{k'=-\infty}^{\infty}\tilde{h}^{(1)}_{k-k'}\tilde{h}^{(2)}_{k'} \tag{25}$$

Graphical interpretation of the convolution product: If we imagine a graphical interpretation of the *spectrum* of a periodic function $h(x) = \sum_{k=-\infty}^{\infty}\tilde{h}_k e^{-2\pi i f_k x}$ (the representation of the function $h(x)$ in k-space given by its Fourier series) as a graph of impulses (δ-distributions) at k scaled by h_k, we can represent the convolution product $H(x)$ as defined above as follows: we consider the spectrum of $h^{(1)}(x)$ (WLOG since convolution is clearly commutative by the above) as described above. We then consider the spectrum of $h^{(2)}(x)$, reflect it with respect to k (i.e. $k \mapsto -k$) and offset it by k' (i.e. $k \mapsto k + k'$). We then superpose the two spectra, multiply the scaling factors of the impulses superposed at every k, and sum the products over k to obtain $H_{k'}$ (Note: in the limit of continuous spectra given by the Fourier transform, this sum becomes an integral represented in the above by the area under the product of the superposed spectra described above).

Example (smooth $h^{(1)}_k$ centered at $k = 0$, $h^{(2)}_k = \delta_{k,50}$):

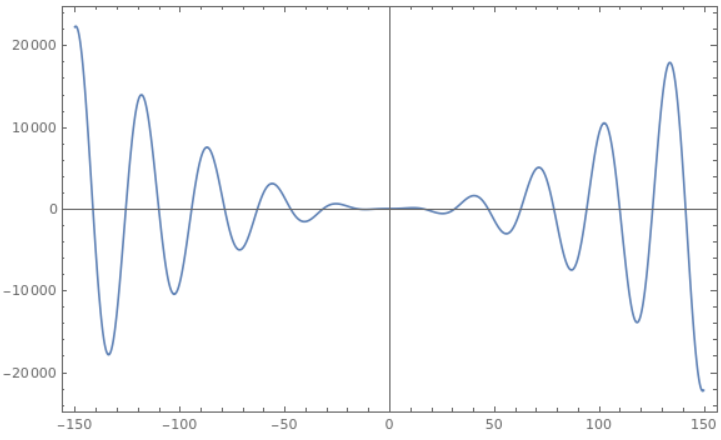

Figure 1: $\tilde{h}^{(1)}_k$

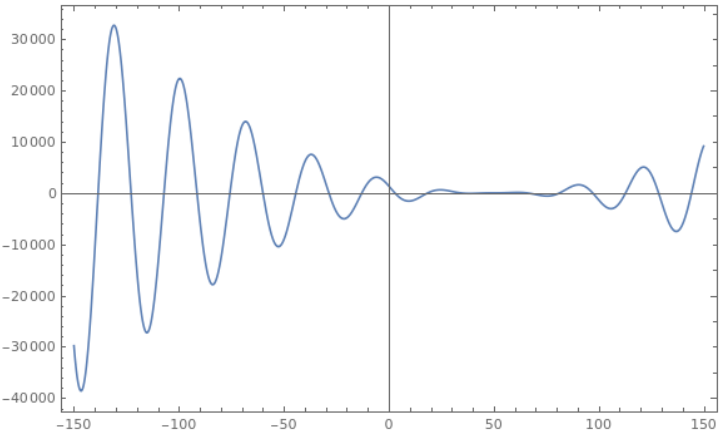

Figure 2: $\tilde{H}_k$

We observe that the convolution is simply the spectrum $h^{(1)}_k$ shifted forwards by 50 (i.e., $\tilde{H}_k = h^{(1)}_{k-50}$).

5. We test the numpy fft function by first working out the expected spectrum for a function (in our case a cosine then a Gaussian) and observing whether the fft output matches our expected spectrum. Then we use the inverse fft (ifft in numpy) to recover our function and verify that we actually recover our input.

   Cosine function: For a function of the form $C + A\cos(ft + \varphi)$, we expect the spectrum to be two delta peaks, one at $f = 0$ corresponding to the offset C, and the other at frequency f. When displaying the spectrum, we will be plotting the absolute values of the Fourier coefficients h_k, and therefore our spectrum plot will disregard any phase shift φ since phase shift will change the complex value of h_k but not it's absolute value (i.e. it will rotate the phasor corresponding the h_k in the complex plane.

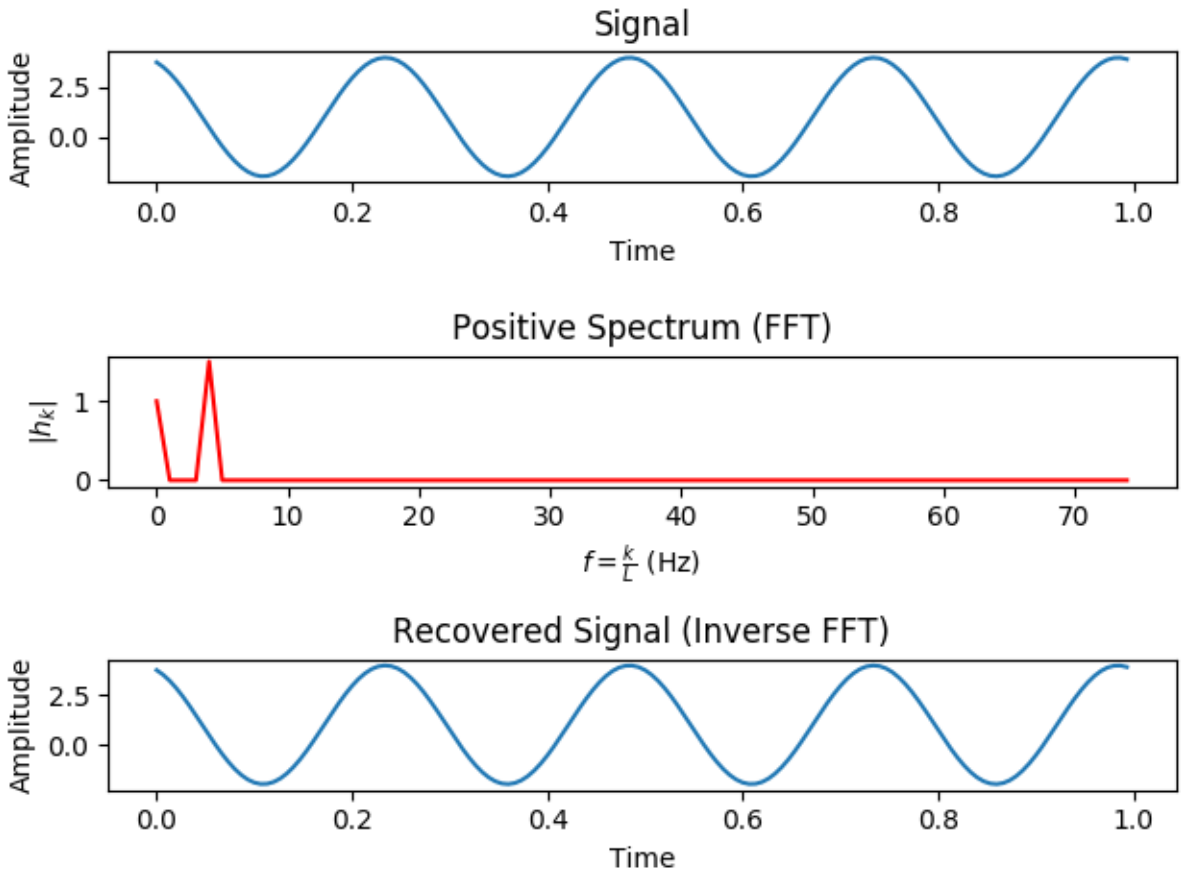

Figure 3: Plot of the signal $h(t) = 1 + 3\cos(4t + 0.1)$, its spectrum, and the signal recovered from the spectrum using the inverse FFT. All the expected features mentioned above are observed, indicating a successful test of numpy's FFT. The amplitudes of the peaks in the spectrum correspond to the absolute values of h_k.

Gaussian function: First, we find the Fourier series of the Gaussian function $h(t) = Ae^{-B(t-\frac{L}{2})^2}$:

$$\tilde{h}_k = \frac{1}{L}\int_0^L h(t)e^{2\pi i f_k t}\,\mathrm{d}t \tag{26}$$

$$= \frac{1}{L}\int_0^L Ae^{-B(t-\frac{L}{2})^2}e^{2\pi i f_k t}\,\mathrm{d}t \tag{27}$$

$$= \frac{1}{L}\int_{-\frac{L}{2}}^{\frac{L}{2}} Ae^{-Bt^2}e^{2\pi i f_k (t+\frac{L}{2})}\,\mathrm{d}t \tag{28}$$

$$= \frac{1}{L}\int_{-\frac{L}{2}}^{\frac{L}{2}} Ae^{-Bt^2}e^{2\pi i f_k t}e^{\pi i k}\,\mathrm{d}t \tag{29}$$

$$= \frac{e^{\pi i k}}{L}\int_{-\frac{L}{2}}^{\frac{L}{2}} Ae^{-Bt^2}e^{2\pi i f_k t}\,\mathrm{d}t \tag{30}$$

$$= \frac{e^{\pi i k}}{L}\int_{-\frac{L}{2}}^{\frac{L}{2}} Ae^{-Bt^2}[\cos(2\pi f_k t) + i\sin(2\pi f_k t)]\,\mathrm{d}t \tag{31}$$

$$= \frac{Ae^{\pi i k}}{L}\left[\int_{-\frac{L}{2}}^{\frac{L}{2}} e^{-Bt^2}\cos(2\pi f_k t)\,\mathrm{d}t + i\int_{-\frac{L}{2}}^{\frac{L}{2}} e^{-Bt^2}\sin(2\pi f_k t)]\,\mathrm{d}t\right] \tag{32}$$

$$= \frac{Ae^{\pi i k}}{L}\int_{-\frac{L}{2}}^{\frac{L}{2}} e^{-Bt^2}\cos(2\pi f_k t)\,\mathrm{d}t \tag{33}$$

$$= \frac{Ae^{\pi i k}}{L}\int_{-\infty}^{\infty} e^{-Bt^2}\cos(2\pi f_k t)\,\mathrm{d}t \tag{34}$$

$$= \frac{Ae^{\pi i k}}{L}\sqrt{\frac{\pi}{B}}e^{\frac{-\pi^2 f_k^2}{B}} \tag{35}$$

$$= \begin{cases} \sqrt{\frac{\pi A^2}{BL^2}}e^{\frac{-\pi^2 k^2}{BL^2}} & k \text{ is even} \\ -\sqrt{\frac{\pi A^2}{BL^2}}e^{\frac{-\pi^2 k^2}{BL^2}} & k \text{ is odd} \end{cases} \tag{36}$$

where in line (28) we have used the change of variables $t \mapsto t + \frac{L}{2}$, in line (31) we used DeMoivre's theorem, in line (33) we used the fact that the second term in line (32) has an odd integrand (the exponential factor is clearly even, and sin is odd so their product is odd) and therefore integrates to zero over symmetric bounds, in line (34) we have changed the bounds by taking the approximation that for $B >> L$ ('B large enough' as mentioned in the question) the Gaussian goes to zero near the bounds and outside, and finally in line (35) we look up the integral (found on Wolfram Mathworld).

We can then expect that the spectrum of the Gaussian is even and oscillates between positive and negative values depending on the parity of k as described above, with amplitude decaying as a scaled Gaussian centered at 0 with increasing absolute value of k . Furthermore, the absolute value spectrum of a Gaussian should be a scaled Gaussian centered at 0.

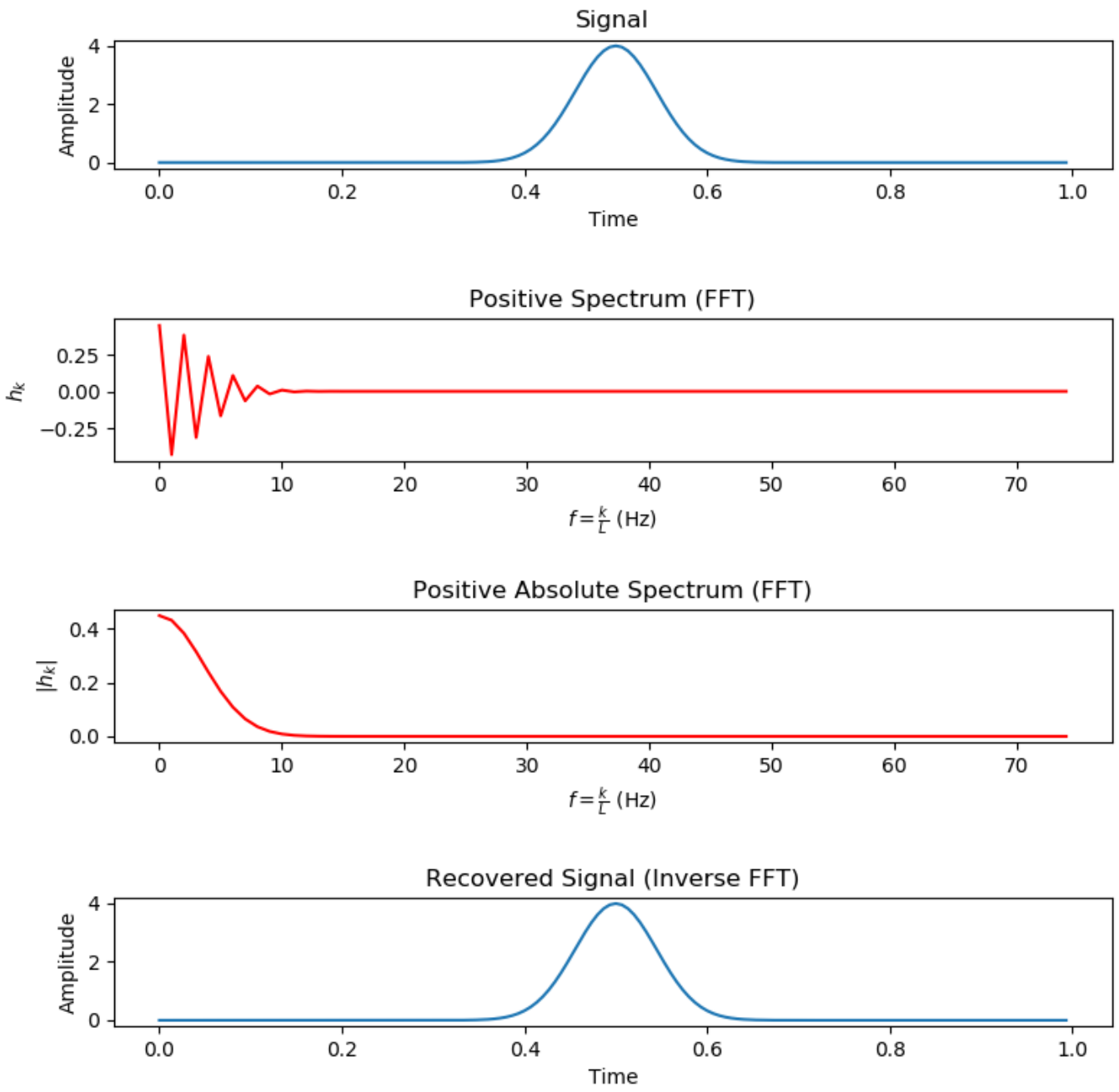

Figure 4: This is for a Gaussian with $A = 4$ and $B = 250$. As expected, the spectrum oscillates between positive and negative values with decaying amplitude with increasing absolute value of k, and the absolute value spectrum is simply a scaled Gaussian. The signal is recovered by the Inverse FFT as desired. From our work above, we calculate an expected value for h_0 of 0.44840, and this is almost exactly the value we observe on our spectrum by printing the 0^{th} element of the FFT array. This indicates another successful test of numpy's FFT.

2 Analysis of Arecibo Data

1. The Fourier spectrum for Arecibo Data is shown below:

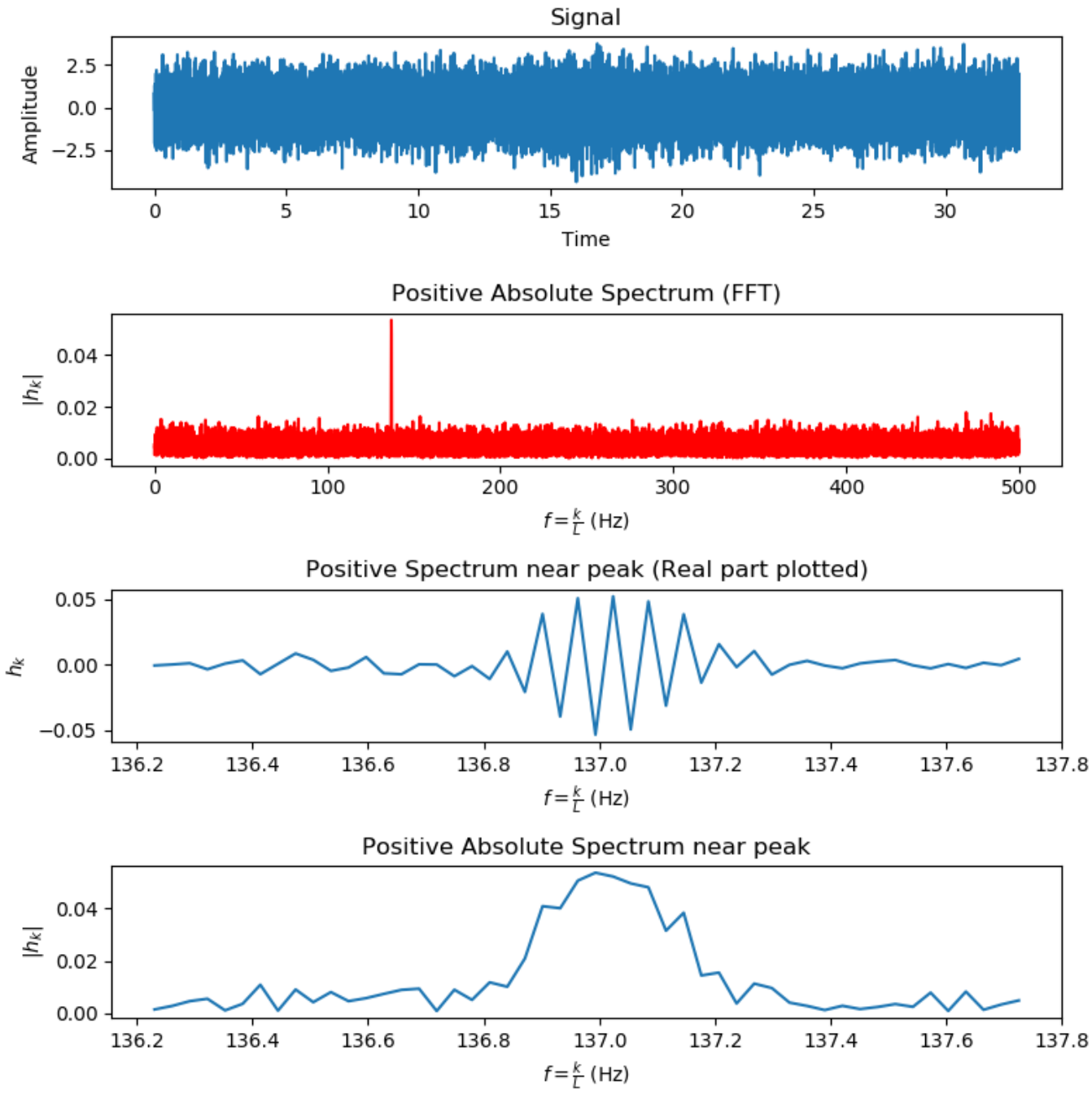

Figure 5: Plots of Arecibo data in time-domain and frequency-domain (the latter obtained using FFT) showing a peak and global maximum at 1420.000137 MHz (recall that the frequencies in the spectrum above are shifted backwards by 1420 MHz). Observe that we do not obtain a sharp peak in the absolute-value spectrum at the signal frequency as we would have for a sinusoidal signal; we obtain a rather rounded peak around the maximum, reminescent of a shifted Gaussian. This is also supported by the oscillation around the peak in the (non-absolute) spectrum.

2. As mentioned above, the shape of the Fourier spectrum peak is indicative of a shifted Gaussian. We therefore attempt a Gaussian+Constant fit using CurveFit (Mathematica package provided for sophomore labs) and obtain the following:

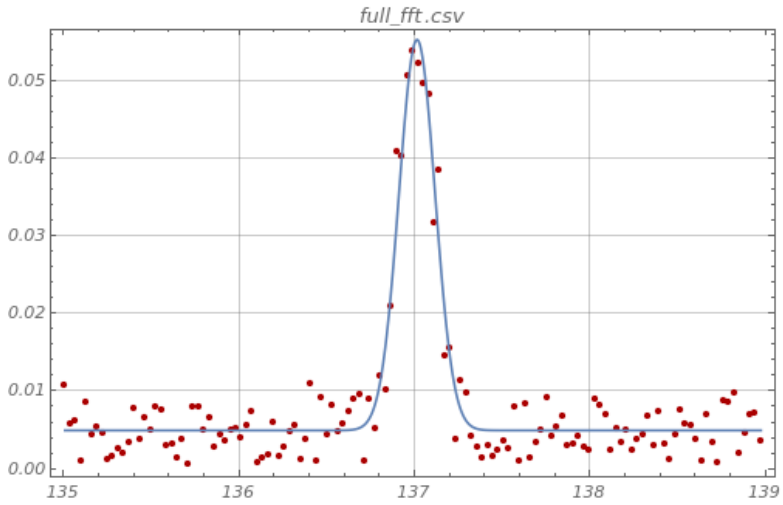

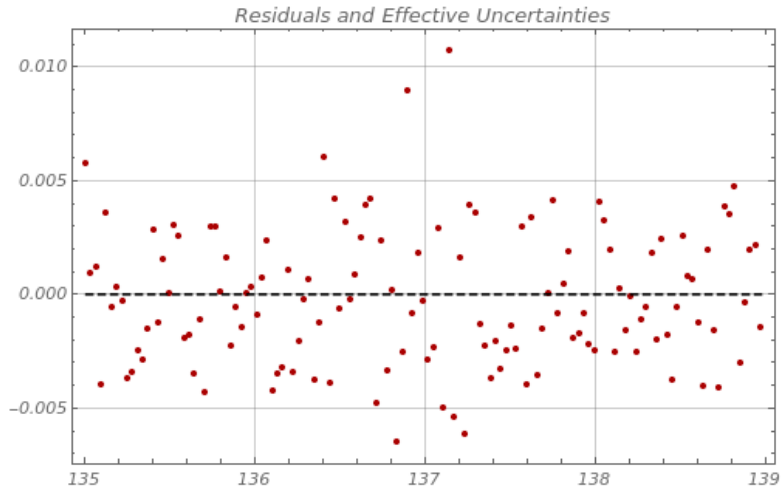

$y(x) =$

$$y_{max} \exp\left(\frac{-(x-\mu)^2}{2\,sigma^2}\right) + c$$

$y_{max}=$ 0.0503238	$c=$ 0.00490238	
$\sigma_{y_{max}}=$ 0.00127453	$\sigma_c=$ 0.000020003	
$\mu=$ 137.016	sigma= 0.102836	
$\sigma_\mu=$ 0.00275514	$\sigma_{sigma}=$ 0.00294051	Std. deviation= 0.00255318

Figure 6: Plot of fit and fit parameters for a Gaussian+Linear fit on our absolute value Fourier spectrum obtained using Curvefit. Peak is found as expected at 1420.000137 MHz, and we observe a qualitatively reasonably good fit (we cannot do a $\tilde{\chi}^2$ or other goodness-of-fit test because we are not given estimates for the uncertainties on our data).

Now, we observe that a shifted Gaussian spectrum can be expressed as the convolution product of a Gaussian spectrum and a delta-peak spectrum. From our work in part I, we can therefore expect the signal to be a Gaussian multiplied by a sinusoidal signal. By a slight modification of our proof for the Fourier spectrum of a Gaussian, we can conclude that knowing t_0, the time about which the Gaussian factor is centered, is not important to finding the time constant Δt of the envelope: to account for general centerings other than $t_0 = \frac{L}{2}$, we simply have to modify the complex exponential factor in our result, and obtain:

$$\tilde{h}_k = e^{2\pi i f_k t_0} \sqrt{\frac{\pi A^2}{BL^2}} e^{\frac{-\pi^2 f_k^2}{B}}$$

which still has absolute value

$$|\tilde{h}_k| = \sqrt{\frac{\pi A^2}{BL^2}} e^{\frac{-\pi^2 f_k^2}{B}}$$

as before. Therefore, we can use our fit parameters for the absolute-value spectrum of our data to estimate Δt by equating the variances as follows:

$$\frac{\pi^2}{B} = \frac{1}{2\sigma^2} \tag{37}$$

$$\pi^2 (\Delta t)^2 = \frac{1}{2\sigma^2} \tag{38}$$

$$\Delta t = \frac{1}{\sqrt{2}\pi\sigma} \tag{39}$$

$$= 2189\ ms \tag{40}$$

We visually verify our estimate by superposing a plot of the signal's FFT obtained above with the FFT of a Gaussian envelope with $\Delta t = 2.189\ s$.

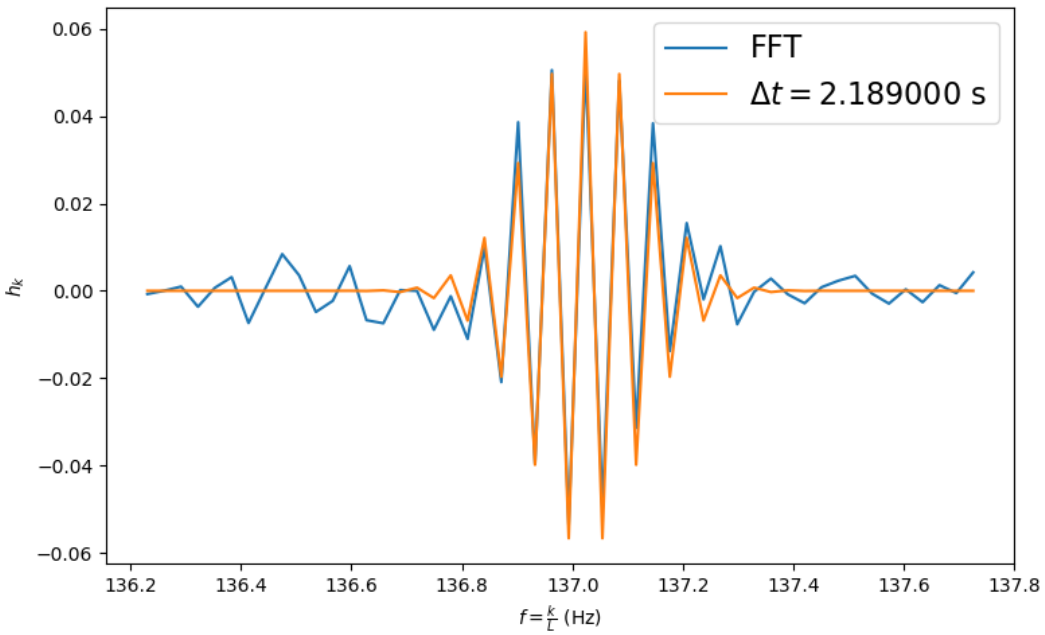

Figure 7: Superimposed plots of the real part of the Fourier spectrum of our signal, and of the spectrum of a Gaussian envelope with $\Delta t = 2.189\ s$. Note that the FFT of the Gaussian has been shifted to account for the convolution with a delta peak at the signal frequency such that our plots coincide as observed. Furthermore, we have roughly scaled the FFT of the Gaussian such that it is easier to make a visual comparison using the superposition.

We observe that our predicted envelope matches quite well with the width of the FFT of our signal, indicating that our guess for $\Delta t = 2.189\ s$ was resonably accurate. For comparison, we present a similar plot with a range of Δt's.

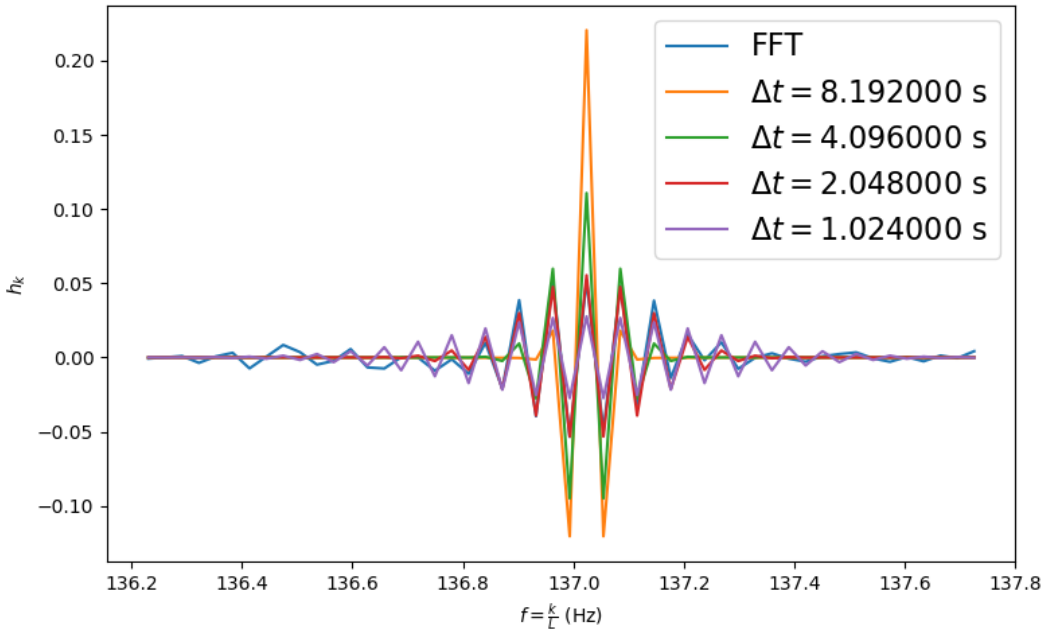

Figure 8: Superimposed plots of the real part of the Fourier spectrum of our signal, and of the spectrum of appropriately shifted and scaled Gaussian envelopes with Δt's as labelled. We can observe that the best match between the envelopes and the FFT of our signal occurs for $\Delta t = 2.05\ s$, i.e. when Δt is the closest to our estimate. However, it is still apparent by comparing with the plot above that our estimate produces the best match between the predicted envelope and the FFT of our signal.

3 Unequally Sampled Data and the Lomb-Scargle Algorithm

1. We use the astropy implementation of the Lomb-Scargle algorithm given by *astropy.stats.LombScargle*.
2. We obtain Lomb-Scargle periodograms of some constructed equally sampled datasets for comparison with the FFT absolute-value spectra we have obtained:

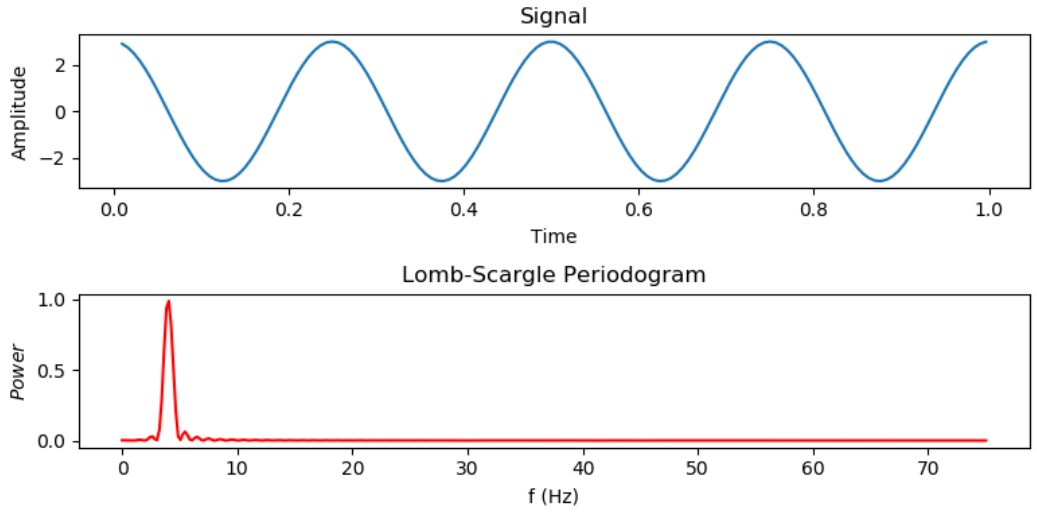

Figure 9: We obtain the Lomb-Scargle periodogram of the signal $h(t) = 1 + 3\cos(4t + 0.1)$. As expected, we see a peak at the 4 Hz position on the periodogram, just as we observed on the FFT absolute-value spectrum of this signal (see Part I.5). However, the Lomb-Scargle algorithm we are using cannot handle zero-frequency terms and therefore we have to diregard any offset in the signal when taking the periodogram; we do not observe the zero-frequency peak we observed on the FFT.

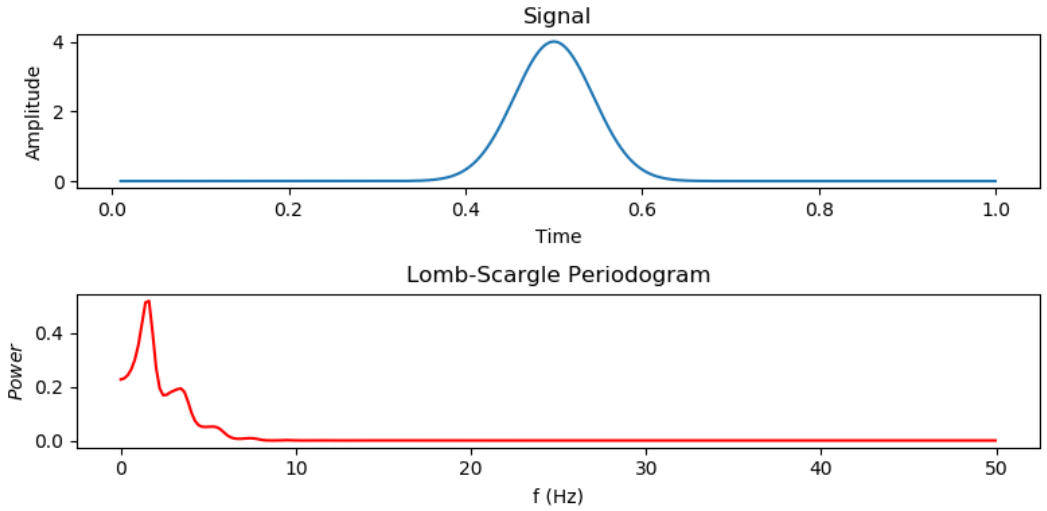

Figure 10: We obtain the Lomb-Scargle periodogram of the Gaussian signal $h(t) = Ae^{-B(t-\frac{L}{2})^2}$ with $A = 4$ and $B = 250$. We observe features in the periodogram in the same region as in the FFT of this signal (see part I.5), as we would expect, but this time the features are heavily distorted with respect to the scaled Gaussian centered at zero that we obtained for the FFT.

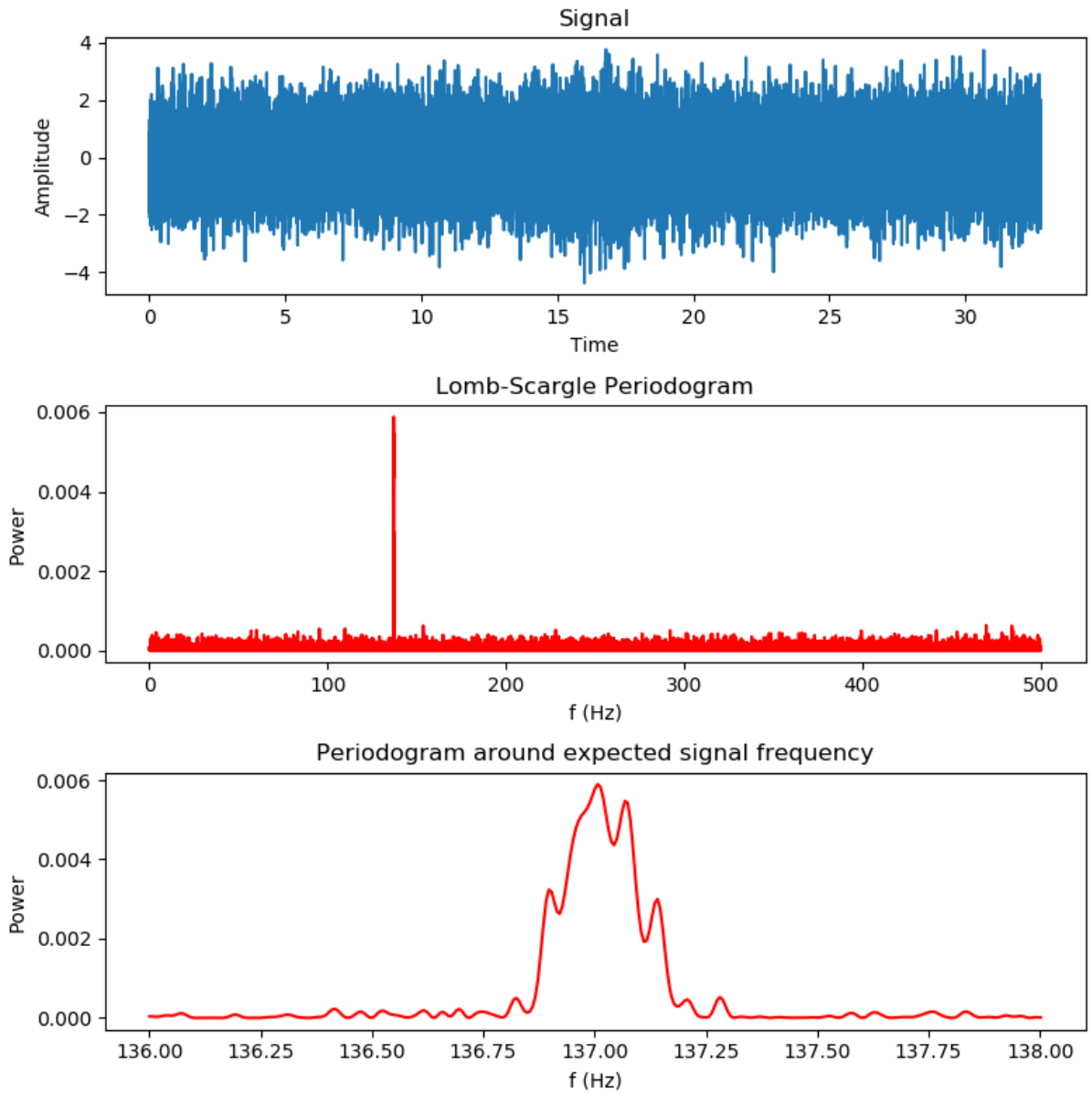

Figure 11: We obtain the Lomb-Scargle periodogram of the Arecibo data analyzed above (part II.4). As expected from the FFT spectrum, we observe a peak at the 1420.000137 MHz frequency (again, remember that our frequency-axis is shifted backwards 1420 MHz). We observe that in the periodogram, the Gaussian envelope appears to cause some distortion in the peak, but does not show up as the characteristic scaled and shifted Gaussian feature observed at the peak in the FFT spectrum.

3. We grab and parse the data for source Her X-1 from the Catalina Real Time Survey using the *vo.table* approach from Assignment 1. We then obtain a Lomb-Scargle periodogram of the data:

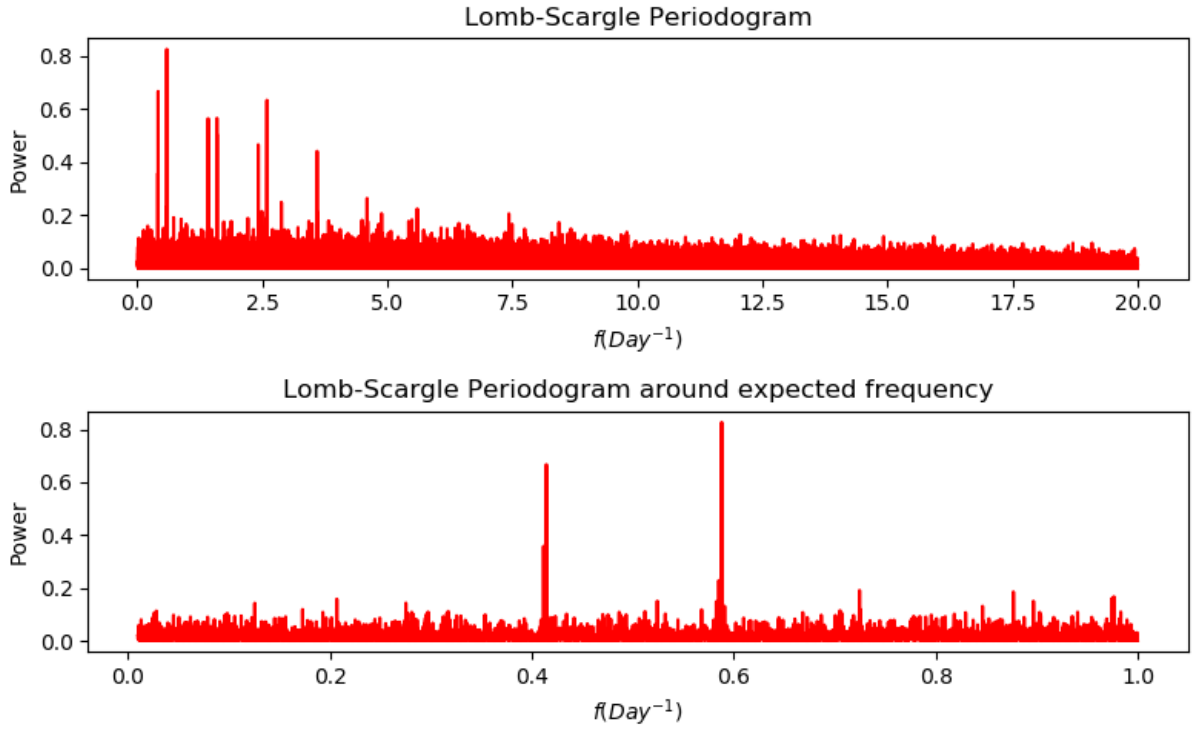

Figure 12: As expected, we find the orbital period of 1.70 days, showing up on the periodogram as the largest peak occuring at $f = \frac{1}{1.70}\ Day^{-1} = 0.588\ Day^{-1}$. We also find a number of less prominent peaks, possibly corresponding to frequency shift, irregular sampling windows, higher-order harmonics occuring due to the signal not being sinusoidal, duplicated peaks due to some asymmetry in the signal, and beats between significant frequencies.

Finally, we confirm that we have found the correct first harmonic for our signal by folding our data around a period of 1.70 days (i.e. we collapse our dataset onto a single period, taking care to propagate uncertainties):

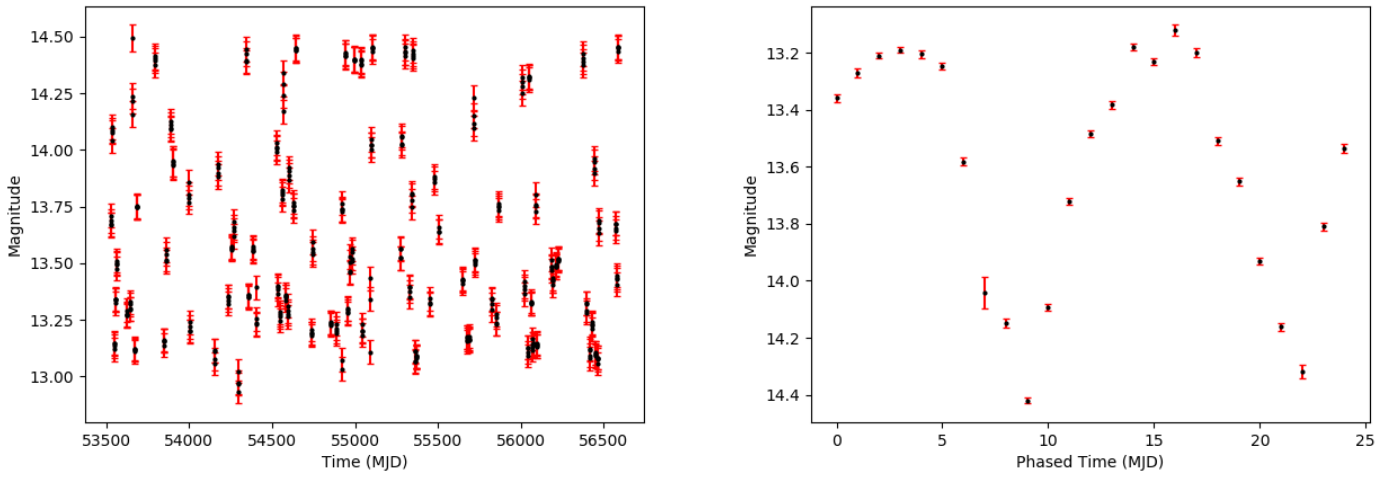

(a) Her X-1 original data.

(b) Folded Her X-1 data (two periods plotted for convenience).

Figure 13: The data folded around a period of 1.70 days closely resembles what we would expect for the lightcurve of an eclipsing binary star system, confirming that we have found the correct first harmonic (i.e. the orbital period of our binary star system).